Quark coalescence and charm(onium) in QGP

R. Rapp[a]

Cyclotron Institute and Physics Department, Texas A&M University, College Station, TX 77843-3366, USA

Abstract. The potential of heavy quarks as probes of the environment produced in hadronic and heavy-ion reactions is discussed. A key role is played by coalescence processes and/or resonance formation in the Quark-Gluon Plasma which are promising candidates to provide a comprehensive understanding of phenomena associated with reinteractions of both open and hidden heavy-quark states.

PACS. 12.38.Mh, 25.75.-q, 14.40.Lb

1 Introduction

In hadronic and heavy-ion collisions, heavy quarks ($Q = c, b$) are believed to be (almost) exclusively pair-produced ($Q\bar{Q}$) upon first impact in hard partonic collisions [1]. This renders them excellent agents of the subsequently formed medium and their reinteractions within. The latter include
(a) coalescence with surrounding quarks as hadronization mechanism in addition to fragmentation, thereby probing the chemical and kinematic properties of the medium [2–6];
(b) energy loss of high-momentum Q-quarks [7,8], which, with increasing interaction strength toward lower momentum, eventually leads to
(c) thermalization [9–12];
and, if the latter can be established,
(d) in-medium dynamics of open and hidden heavy-flavor states [13–17], which is particularly exciting in view of recent QCD lattice calculations [18–20] indicating the survival of low-lying charmonia well into the quark-gluon plasma (QGP).

In this paper we will address the above issues essentially in that order.

2 Coalescence in hadronic collisions

In elementary hadronic reactions (pN, πN) evidence for reinteractions of c-quarks arises from (large) flavor asymmetries in D-meson production yields. The asymmetries are most pronounced at forward rapidities (or x_F), and are successfully attributed to coalescence of c-quarks with valence quarks of the projectile [4]. The pertinent recom-

[a] e-mail: rapp@comp.tamu.edu

bination cross section can be written as [2]

$$x^* \frac{\mathrm{d}\sigma_D^\mathrm{rec}}{\mathrm{d}x_\mathrm{F}} = \int \frac{\mathrm{d}x_{\bar{q}}}{x_{\bar{q}}} \int \frac{\mathrm{d}z}{z} \left(x_{\bar{q}} z^* \frac{\mathrm{d}^2\sigma^{(c\bar{q})}}{\mathrm{d}x_{\bar{q}}\mathrm{d}z} \right) \mathcal{R}(x_q, z; x_\mathrm{F}) \, , \tag{1}$$

where the main elements are
(i) the c–$\bar{q}$ production cross section composed of a 2-parton distribution function (2-PDF), $f_{i\bar{q}}^{(2)}$ (where $i = g, q, \bar{q}$ participates in the hard process to produce the $c\bar{c}$ pair), and the standard perturbative QCD (pQCD) $c\bar{c}$ cross section, and
(ii) the c–$\bar{q} \to D$ recombination function, $\mathcal{R}$.

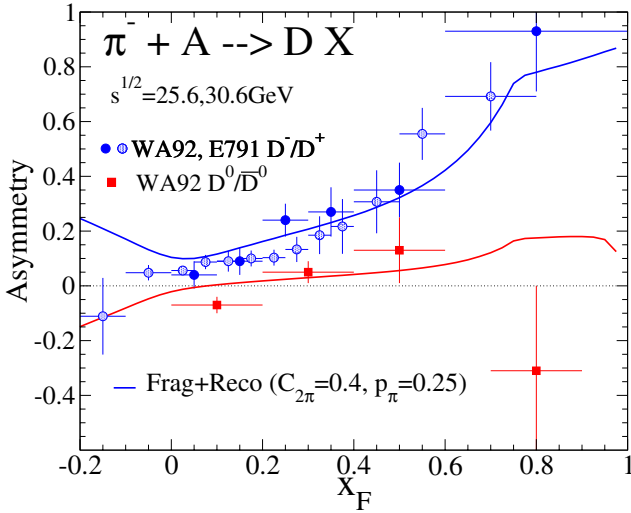The 2-PDF is usually factorized into two single PDFs with phase space correction,

$$f_{i\bar{q}}^{(2)} = C f_{\bar{q}}(x_{\bar{q}}) \, f_i(x_i) \, (1 - x_{\bar{q}} - x_i)^p \, , \tag{2}$$

whereas $\mathcal{R}$ represents a D-meson wave function which in [6] has been assumed to be Gaussian in rapidity space,

$$\mathcal{R}(y_{\bar{q}}, y_c, y) = \exp(\Delta y^2/2\sigma_y^2)/\sqrt{2\pi\sigma_y^2} \, . \tag{3}$$

This form of the recombination function [21] allows one to generalize the coalescence formalism to include sea quarks [6], and thus address flavor asymmetries also at central x_F; cf. Fig. 1. The experimentally observed asymmetries in inclusive yields ($x_\mathrm{F} > 0$) are quite appreciable, e.g., $D^-/D^+ = 1.35 \pm 0.05$ (versus 1 in isospin-symmetric fragmentation), $D^0/\bar{D}^0 = 0.93 \pm 0.03$ (versus 1) and $D^\pm/(\bar{D}^0 + D^0) = 0.415 \pm 0.01$ (versus 0.33) for fixed-target $\pi^- N$ collisions (averaged over a weak energy dependence for $\sqrt{s} = 19$–$34\,\mathrm{GeV}$) [23]. The data are rather well reproduced by a combined coalescence + fragmentation approach [6] (for a somewhat different framework based on power corrections, see [5]).
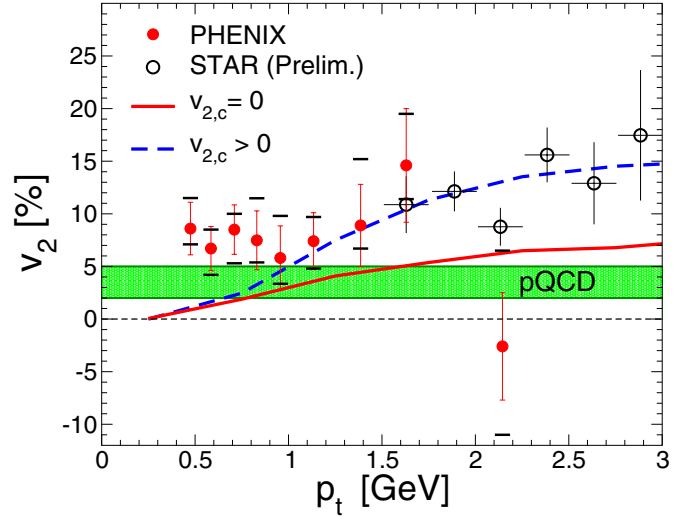
Fig. 1. D-meson flavor asymmetries, $A = (N_{D_1} - N_{D_2})/(N_{D_1} + N_{D_2})$, in $\pi^- - A$ reactions [22,23] compared to coalescence + fragmentation calculations [6]. Upper data points and curves are for $D_1 = D^-$ and $D_2 = D^+$, whereas lower data points and curves are for $D_1 = D^0$ and $D_2 = \bar{D}^0$. "Leading" particles ($D^- = \bar{c}d$, $D^0 = c\bar{u}$) are defined as sharing a valence quark with the projectile ($\pi^- = d\bar{u}$); note that the approximate absence of an asymmetry for $D^0/\bar{D}^0$ is accounted for in the model due to the predominant production of $c\bar{c}$ pairs in the forward direction via $\bar{u}u$ annihilation, rendering the valence $\bar{u}$ unavailable for recombination

Fig. 2. Azimuthal asymmetry of "non-photonic" single-$e^\pm$ spectra in minimum bias Au–Au ($\sqrt{s_{NN}} = 200\,\text{GeV}$) [28,29] compared to coalescence model predictions [25] using c-quark distributions from either p–p collisions ($v_2^c = 0$, solid line) or assuming a transverse flow and v_2-profile as determined for light quarks from fits to light-hadron spectra ($v_2^c > 0$, dashed line). The band indicates predictions from jet-quenching [24] applicable at sufficiently high p_t

3 Open charm in the QGP

Final-state interactions of heavy quarks are enhanced when embedding them into a heavy-ion collision, where, at ultrarelativistic energies, intense reinteractions of light partons are believed to form locally thermalized matter within a time of $\tau \lesssim 1\,\text{fm}/c$. At high momenta c-quarks rescatter perturbatively inducing a softening of the primordially power-like p_t spectra, with subsequent hadronization in the vacuum (fragmentation). The predicted suppression factors relative to p–p collisions range from 0.2 [8] to 0.5 [7], with a rather small azimuthal asymmetry, $v_2 \leq 5\%$ [24].

Toward lower p_t, the phase space density of the medium increases and coalescence with light quarks is expected to become competitive [25–27]. The same expression, (1), can be applied with the light quark distributions being replaced by thermal (+ quenched pQCD) ones as established from light hadron production systematics (also, the recombination function $\mathcal{R}$ is typically substituted with a hadron wave function in transverse momentum). The extension to low p_t is, in principle, more controlled than for light–light (q–$\bar{q}$) coalescence, since at the scale of the hadronization temperature, secondary c production is negligible. With previously determined light-quark distributions, charmed-hadron spectra become a sensitive probe of the dynamics of c-quarks in the QGP. This has first been quantified in the context of "charm-like" single-electron spectra in [25], showing that $v_2^e(p_t)$
(a) closely reflects the v_2 of the parent D-meson,

(b) exhibits a marked difference of more than a factor of 2 between the cases where the c-quark distributions are either taken from p–p collisions, or assumed to follow the systematics of light quarks (including collective expansion); cf. Fig. 2.

Current data at RHIC from PHENIX [28] and STAR (preliminary) [29] seem to favor the quasi-thermalized scenario. If confirmed, this raises at least two further questions:
(i) Is the predicted v_2^e consistent with pertinent p_t spectra (i.e., the ratio of central Au–Au to collision-scaled p–p spectra, R_{AA})?
(ii) What are microscopic mechanisms for thermalization of c-quarks (or D-mesons)?

Concerning (i), it has been pointed out [30] that for single-$e^\pm$ p_t spectra in central Au–Au, N_{coll}-scaled D-meson spectra from p–p collisions lead to results rather similar to a scenario based on full thermalization and collective flow close to hadronic freeze-out ($T \simeq 130\,\text{MeV}$, $v_\perp = 0.65$), due to large blue shifts with $m_D = 1.87\,\text{GeV}$ (also, bottom-decay contributions become significant above $p_t^e \simeq 3\,\text{GeV}$). However, in hydrodynamic analysis [12] coupled with a Fokker–Planck treatment of c-quarks in the QGP, a v_2^c of ~ 10–15% is associated with $R_{AA}^c(p_t \geq 3\,\text{GeV}) \leq 0.1$. Coalescence model calculations [25], based on recombination at the phase boundary, imply a suppression factor similar to jet quenching, $R_{AA}^D(p_t \simeq 3\,\text{GeV}) = 0.2$–0.5, but with $v_2^D(p_t \simeq 3\,\text{GeV}) \simeq 15\%$. Note that starting from c-quark spectra, fragmentation leads to a degradation, whereas coalescence to an increase, of the resulting D-meson p_t.
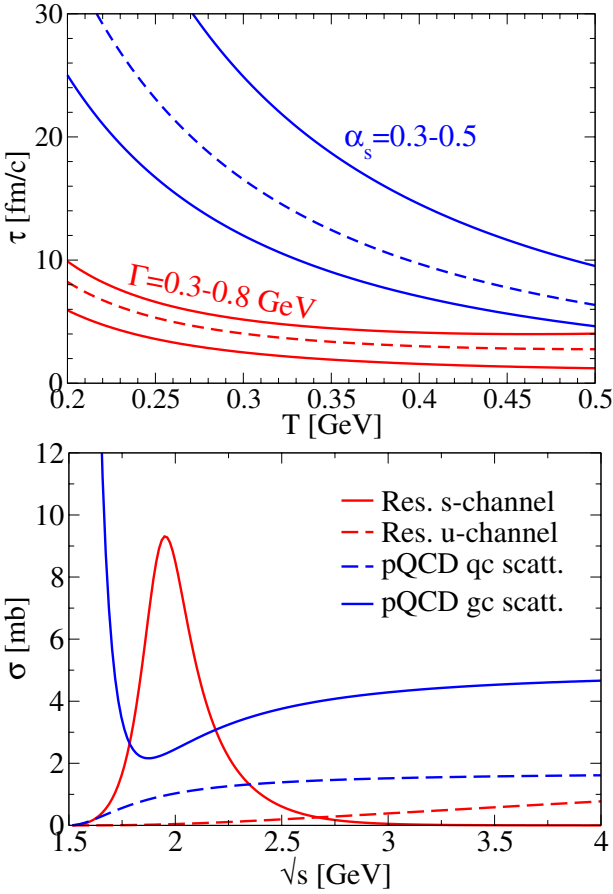
Fig. 3. Upper panel: c-quark equilibration times in QGP with pQCD interactions (upper band; upper [lower] line corresponds to $\alpha_s = 0.3[0.5]$) and when adding "D"-meson resonance rescattering (lower band; the range of resonance widths indicates variations in the coupling constant of the c–q–D vertex with the upper [lower] line corresponding to $\Gamma_D = 0.3[0.8]$ GeV) [11]. Lower panel: underlying total c-parton cross sections

Concerning (ii), it has been known for a while [9] (and confirmed in [10,11]) that perturbative c-quark rescattering off quarks and gluons in the QGP implies kinetic relaxation times $\tau_c^{\mathrm{therm}} \gtrsim 10$ fm/c for $T \simeq 400$ MeV, too long to achieve thermalization at RHIC. However, as shown recently [11], nonperturbative rescattering in the QGP can lead to a substantial acceleration of equilibration: implementing the notion of D-meson-like resonances within a Fokker–Planck equation, a reduction of τ_c^{therm} by a factor of ~ 3 as compared to using pQCD cross sections has been found (for $T \leq 2T_c$); cf. upper panel of Fig. 3 (similar for b-quarks, but with absolute values $\tau_b^{\mathrm{therm}} \simeq 4\tau_c^{\mathrm{therm}}$). The main difference in the two mechanisms resides not so much in the total cross sections (lower panel of Fig. 3), as in the isotropic angular distribution for the resonance case as opposed to forward-dominated pQCD scattering. It has also been noted [11] that the efficiency of this mechanism relies to a significant part on the D-states being located *above* the c–q threshold (i.e., not being bound states, which renders them inaccessible in $2 \to 2$ scattering, especially due to the thermal energies carried by the light quarks). It will be very valuable to check this in QCD lattice calculations, as well as whether previously found q–$\bar{q}$ and Q–$\bar{Q}$ states carry over to the Q–$\bar{q}$ sector. Furthermore, an increasing population of (colorless) "hadronic" states in the cooling process toward T_c could serve as a mechanism to put phenomenologically successful coalescence models on a firmer basis (also in the light-quark sector). The in-medium mass of open-charm states in the QGP also bears on the production of charmonia, as will be seen in the following section.

From a phenomenological point of view, it should be kept in mind that any process contributing to elastic c-quark scattering in the QGP, $c + X_1 \to c + X_2$, in principle also gives rise to secondary $c\bar{c}$ production in the crossed channel, $X_1 + \bar{X}_2 \to c + \bar{c}$, which can be constrained experimentally by total $c\bar{c}$ yields (including nontrivial centrality dependencies). For instance in [27] it has been pointed out that when upscaling the perturbative $gc \to gc$ cross section by a factor of 3 (to generate an elliptic flow comparable to light quarks), secondary charm production is at the 40–50% level of the primordial yield in central Au–Au ($\sqrt{s} = 200$ AGeV). This is expected to be less pronounced for heavier exchange particles, such as "D"-mesons.
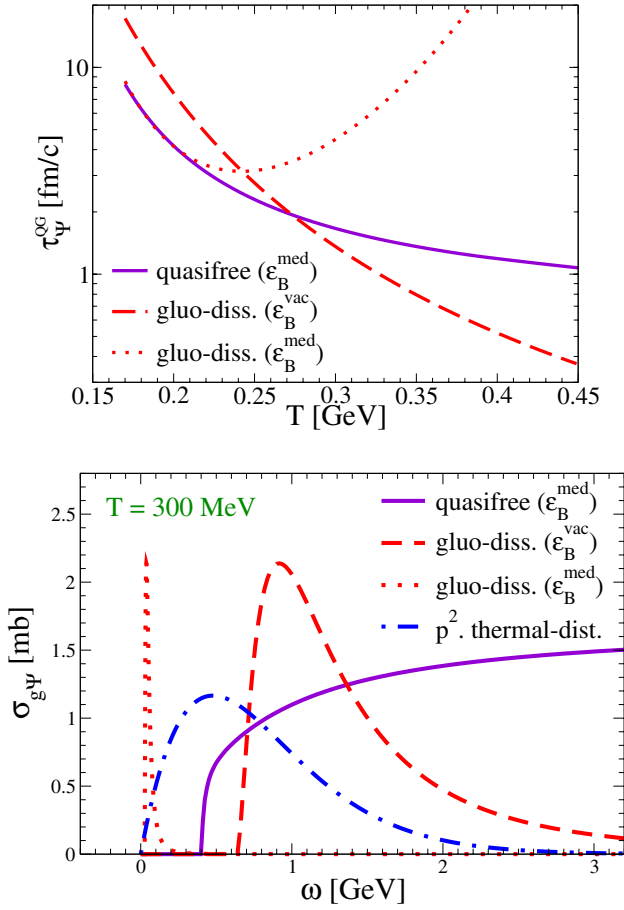
4 Charmonium in the QGP

A central quantity in evaluating medium effects on quarkonium states, Ψ, in a heavy-ion collision are their inelastic cross sections, $\sigma_\Psi^{\mathrm{diss}}$, with partons in the QGP, determining the pertinent dissociation rate as

$$\Gamma_\Psi = (\tau_\Psi)^{-1} = \int \frac{\mathrm{d}^3 k}{(2\pi)^3} \, f^{q,g}(\omega_k, T) \, v_{\mathrm{rel}} \, \sigma_\Psi^{\mathrm{diss}}(s) \,. \quad (4)$$

A widely used model for $\sigma_\Psi^{\mathrm{diss}}$ is the gluon-absorption break-up [31,32], $g + \Psi \to c + \bar{c}$, characterized by a pronounced maximum at a gluon energy $\omega_{\mathrm{max}} \simeq 1.5\epsilon_{\mathrm{B}}$ (ϵ_{B} is the quarkonium binding energy); see lower panel in Fig. 4. For J/ψ-mesons with their free binding energy, $\epsilon_{\mathrm{B}}^{\mathrm{vac}} = 640$ MeV, ω_{max} essentially coincides with thermal gluon energies, $\omega = 3T$, for $T \simeq 300$ MeV. Debye screening of the Q–$\bar{Q}$ potential in the QGP is, however, expected to substantially reduce ϵ_{B} [34]. This renders gluodissociation an increasingly inefficient process at higher T due to a shrinking break-up kinematics; cf. dotted lines in Fig. 4. For small ϵ_{B}, "quasifree" dissociation [33,15], $g(q, \bar{q}) + \Psi \to c + \bar{c} + g(q, \bar{q})$, albeit naively suppressed by one power of α_s, has been identified as a more important mechanism due to much larger overlap with the thermal (quark + gluon) phase space (cf. solid and dash-dotted lines in the lower panel of Fig. 4).
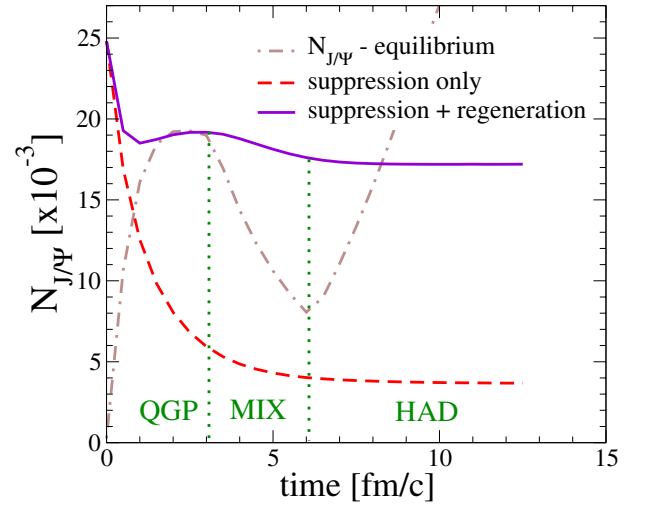
If the number of heavy quarks in a heavy-ion collision is large enough, their recombination into quarkonia could become a significant (or even dominant) contribution to the final yield [35–37,33,38,39]. The conditions for this to happen can be assessed in terms of a simple rate equation for the time evolution of the number of Ψ's,

$$\frac{\mathrm{d}N_\Psi}{\mathrm{d}t} = -\Gamma_\Psi \left(N_\Psi - N_\Psi^{\mathrm{eq}} \right) \,. \quad (5)$$

Fig. 5. Time evolution of the J/ψ abundance in central Au–Au ($\sqrt{s_{NN}} = 200\,\mathrm{GeV}$) based on a solution of the rate (5) in an expanding thermal fireball including in-medium effects on both open and hidden charm mesons [16]. Dashed line: suppression only (no gain term); dash-dotted line: temperature-dependent equilibrium number, $N_{J/\psi}^{\mathrm{eq}}(T;\gamma_c)$; solid line: total number $N_{J/\psi}(t)$
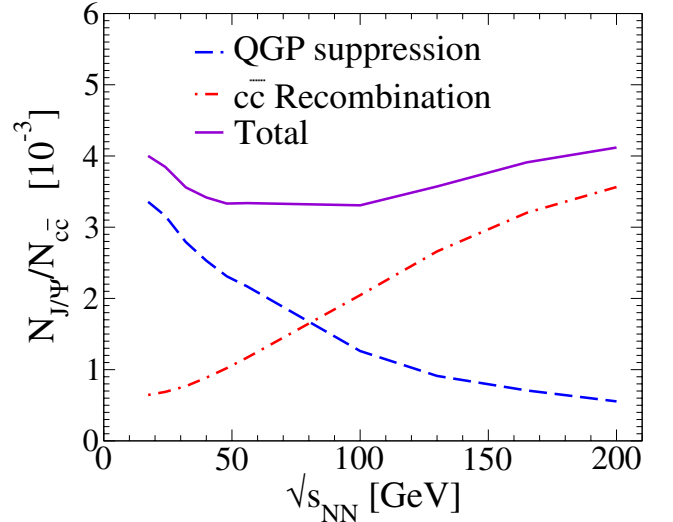

Fig. 4. Upper panel: J/ψ lifetimes in the QGP using gluodissociation [32] with vacuum (dashed line) and in-medium reduced (dotted line) binding energy, as well as quasifree dissociation [33] with in-medium reduced binding energy (solid line). Lower panel: pertinent cross sections (line identification as in upper panel) relative to thermal parton distribution functions (dash-dotted line)
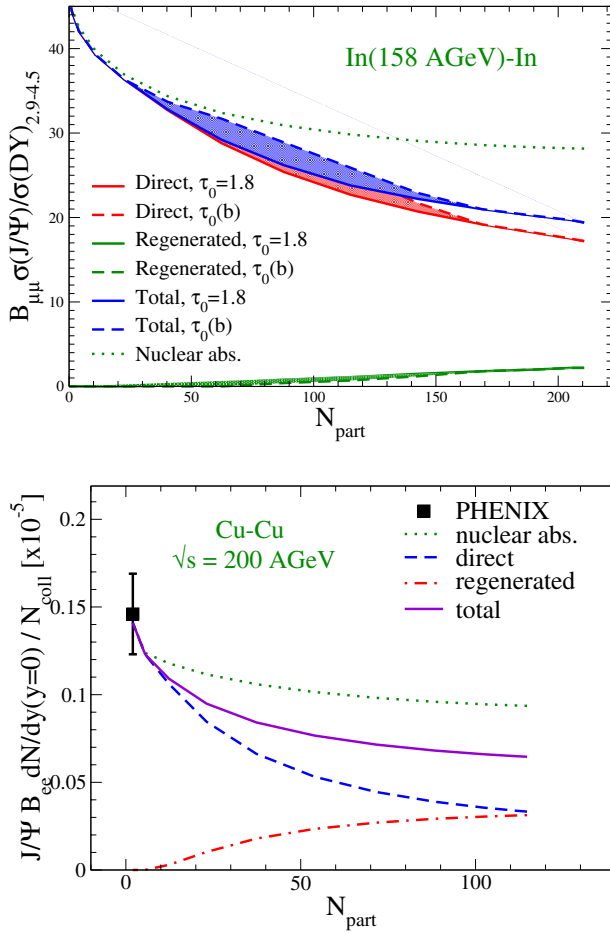

Fig. 6. Theoretical predictions for the excitation function of J/ψ production in central Au–Au collisions. Suppression (dashed line) and regeneration (dash-dotted line) components combine into a rather flat energy dependence for the total yield (solid line) [33]

Besides the reaction rate Γ_Ψ, the other quantity governing the evolution of N_Ψ is the equilibrium abundance, $N_\Psi^{\mathrm{eq}}(T;\gamma_c)$, which determines Ψ regeneration, i.e., the gain term in (5), as required by detailed balance. $N_\Psi^{\mathrm{eq}}(T;\gamma_c)$ is typically evaluated in the canonical ensemble with the total number of (primordial) $c\bar{c}$ pairs fixed via a fugacity $\gamma_c = \gamma_{\bar{c}} = \mathrm{e}^{\mu_c/T}$. This implies that $N_\Psi^{\mathrm{eq}}(T;\gamma_c)$ is sensitive to the open-charm spectrum, in particular (in-medium) masses of c-quarks (or D-mesons) [15,16]; e.g., if m_c^* (or m_D^*) is reduced in matter (with m_Ψ constant), c- and $\bar{c}$-quarks are thermally favored to occur in open-charm states, thus reducing $N_\Psi^{\mathrm{eq}}(T;\gamma_c)$. Finally, the gain term depends on the c-quark momentum distributions; its particularly simple form in (5), based on thermalized c-quarks, illustrates the impact of c-quark rescattering (as discussed in the previous section) on charmonia. Therefore, thermalization of c-quarks opens the window on equilibrium properties of both open and hidden charm, i.e., their masses encoded in $N_\Psi^{\mathrm{eq}}(T;\gamma_c)$, as well as charmonium widths (Γ_Ψ). A sensitive observable to distinguish

direct and regenerated J/ψ's turns out to be their elliptic flow, v_2^Ψ [40,25,41][1]. If only suppression is operative, v_2^Ψ reaches a maximal value of ~ 2–3% [40], while it grows up to $\sim 15\%$ at $p_t^\Psi \simeq 4\,\mathrm{GeV}$ for thermal c–$\bar{c}$ coalescence [25].

A calculation [16] of the time evolution of $N_{J/\psi}$ in central Au–Au ($\sqrt{s} = 200\,\mathrm{AGeV}$) based on (5) including in-medium masses of open-charm and reduced J/Ψ binding energies, as well as incomplete thermalization of

---

[1] I thank B. Müller for raising this question.

Complementary information on the interplay between primordial and secondary J/ψ production can be extracted by going to smaller nuclear collision systems. Pertinent predictions are shown in Fig. 7, reconfirming the absence of noticeable regeneration at SPS (as well as a smooth centrality dependence; upper panel), but an approximately equal amount of primordial and regenerated J/ψ's for central Cu–Cu at RHIC (lower panel).

5 Conclusions

Hadrons containing heavy quarks are excellent probes of the environment formed in nuclear reactions. Evidence for coalescence mechanisms in elementary hadronic reactions finds its natural extension for both D-mesons and charmonia to heavy-ion collisions. In addition, at RHIC, the produced medium appears to interact strongly enough to thermalize c-quarks (but not b-quarks). If confirmed, "D"-meson resonance formation in the QGP (coupled with pertinent coalescence at T_c) might be the key to a simultaneous understanding of (suppressed) p_t spectra and (large) elliptic flow of D-mesons (and single electrons). The transition into a perturbative energy-loss picture could be shifted to higher p_t than for light hadrons. Resonance states in the QGP also have substantial impact on charmonium production, facilitating their regeneration in the 1–$2T_c$ regime where inelastic collision rates are high. Here, thermalization of c-quarks would enable a rather direct window on spectral properties of open and hidden charm, i.e., their masses and widths. Work in progress on Υ production [42] seems to indicate, however, that even at LHC their suppression is prevalent, due to a lack of thermalization of bottom quarks. Thus, a simultaneous observation of Υ suppression and the absence thereof for J/ψ at collider energies would provide strong evidence for secondary charmonium production.

Among the main challenges yet to be met is establishing connections of heavy-quark observables to ("pseudo"-) order parameters of the QCD phase transition [43]. With low-lying charmonia possibly surviving up to $2T_c$, their dissolution evades a direct relation to T_c. A suitable quantity could be their inelastic width, which in model calculations is typically quite different (smaller) in the hadronic compared to the QGP phase [15]. Quenched lattice calculations [20] indicate a similar trend, but unquenching has to be awaited for more definite conclusions. We also mention the recent work of [44], where an increase in transverse-momentum fluctuations of open-charm states has been linked to a first-order transition.

Looking into the future, it seems that the combined experimental and theoretical analysis of heavy-quark observables in ultrarelativistic heavy-ion collisions is on a promising path toward providing a milestone in the identification of the QGP.

Fig. 7. Theoretical predictions for the centrality dependence of J/ψ production in intermediate-size-ion collisions at SPS (upper panel) and RHIC (lower panel), including both suppression and regeneration processes [16]. The bands in the upper panel reflect uncertainties in the formation time which is expected to increase at lower collision centrality (dashed lines)

c-quarks in the early stages, is displayed in Fig. 5. One finds that the J/ψ yield equilibrates close to the phase boundary, with the major contribution arising from regeneration in the QGP and little changes in the "mixed" and hadronic phase. Note that this result crucially hinges on the notion of the J/ψ surviving as a resonance in the QGP under RHIC conditions, $T \leq 2T_c$. The final yield is a factor of ~ 4–5 increased over a scenario with suppression only. The situation is quite different at SPS energies ($\sqrt{s} = 17.3$ AGeV): with an expected open-charm number $N_{c\bar{c}} \simeq 0.2$ in central Pb–Pb, secondary charmonium formation is negligible and J/ψ *suppression* is the main mechanism at work. Obviously, this calls for mapping out the excitation function for $\sqrt{s} = 20$–200 GeV (accessible at RHIC), as suggested in [33]. Based on Fig. 6 one expects a transition from a suppression-dominated regime (SPS or low RHIC energies) to a regeneration-dominated one at $\sqrt{s} \gtrsim 100$ AGeV, resulting in a rather flat energy dependence (possibly with a shallow minimum).

References

1. P. Levai, B. Müller, R. Vogt, Phys. Rev. C **51**, 3326 (1995)
2. V.G. Kartvelishvili, A.K. Likhoded, S.R. Slabospitsky, Sov. J. Nucl. Phys. **33**, 434 (1981)
3. R. Vogt, S.J. Brodsky, P. Hoyer, Nucl. Phys. B **383**, 643 (1992)
4. R. Hwa, Phys. Rev. D **51**, 85 (1995)
5. E. Braaten, Y. Jia, T. Mehen, Phys. Rev. Lett. **89**, 122002 (2002)
6. R. Rapp, E.V. Shuryak, Phys. Rev. D **67**, 074036 (2003)
7. M. Djordjevic, M. Gyulassy, S. Wicks, hep-ph/0410372
8. N. Armesto, A. Dainese, C.A. Salgado, U.A. Wiedemann, nucl-th/0501225
9. B. Svetitsky, Phys. Rev. D **37**, 2484 (1988)
10. M.G. Mustafa, D. Pal, D.K. Srivastava, Phys. Rev. C **57**, 889 (1998)
11. H. van Hees, R. Rapp, Phys. Rev. C (2005), in press, and nucl-th/0412015
12. G.D. Moore, D. Teaney, hep-ph/0412346
13. T. Matsui, H. Satz, Phys. Lett. B **178**, 416 (1986)
14. G. Burau, D. Blaschke, Y.L. Kalinovsky, Phys. Lett. B **506**, 297 (2001)
15. R. Rapp, L. Grandchamp, J. Phys. G **30**, S305 (2004)
16. L. Grandchamp, R. Rapp, G.E. Brown, Phys. Rev. Lett. **92**, 212301 (2004)
17. C.Y. Wong, hep-ph/0408020
18. M. Asakawa, T. Hatsuda, Phys. Rev. Lett. **92**, 012001 (2004)
19. S. Datta, F. Karsch, P. Petreczky, I. Wetzorke, Phys. Rev. D **69**, 094507 (2004)
20. T. Umeda, H. Matsufuru, hep-lat/0501002
21. E. Takasugi, X. Tata, C.B. Chiu, R. Kaul, Phys. Rev. D **20**, 211 (1979)
22. E791 Collaboration (E.M. Aitala et al.), Phys. Lett. B **371**, 157 (1996)
23. Beatrice Collaboration (M. Adamovich et al.), Nucl. Phys. B **495**, 3 (1997)
24. M. Djordjevic, M. Gyulassy, Proceedings of 20th Winter Workshop on Nuclear Dynamics (Trelawny Beach, Jamaica, March 15–20, 2004), edited by W. Bauer et al., EP Systema (Budapest, Hungary, 2004) p. 293
25. V. Greco, C.M. Ko, R. Rapp, Phys. Lett. B **595**, 202 (2004)
26. L.-W. Chen, C.M. Ko, nucl-th/0409058
27. D. Molnar, nucl-th/0410041
28. PHENIX Collaboration (S.S. Adler et al.), nucl-ex/0502009
29. STAR Collaboration (F. Laue et al.), nucl-ex/0411007
30. S. Batsouli, S. Kelly, M. Gyulassy, J.L. Nagle, Phys. Lett. B **557**, 26 (2003)
31. E.V. Shuryak, Sov. J. Nucl. Phys. **28**, 408 (1978)
32. G. Bhanot, M. Peskin, Nucl. Phys. **156**, 391 (1979)
33. L. Grandchamp, R. Rapp, Phys. Lett. B **523**, 60 (2001); Nucl. Phys. A **709**, 415 (2002)
34. F. Karsch, M.T. Mehr, H. Satz, Z. Phys. C **37**, 617 (1988)
35. P. Braun-Munzinger, J. Stachel, Phys. Lett. B **490**, 196 (2000)
36. R.L. Thews, M. Schroedter, J. Rafelski, Phys. Rev. C **63**, 054905 (2001)
37. M. Gorenstein, A.P. Kostyuk, H. Stöcker, W. Greiner, Phys. Lett. B **524**, 265 (2002)
38. B. Zhang, C.M. Ko, B.A. Li, Z.W. Lin, S. Pal, Phys. Rev. C **65**, 054909 (2002)
39. E.L. Bratkovskaya, W. Cassing, H. Stöcker, Phys. Rev. C **67**, 054905 (2003)
40. X.-N. Wang, F. Yuan, Phys. Lett. B **450**, 62 (2002)
41. E.L. Bratkovskaya, W. Cassing, H. Stöcker, N. Xu, nucl-th/0409047
42. S. Lumpkins, L. Grandchamp, D. Sun, H. van Hees, R. Rapp, in preparation (2005)
43. M. Nardi, H. Satz, Phys. Lett. B **442**, 14 (1998)
44. S. Terranova, D.M. Zhou, A. Bonasera, nucl-th/0412031